

ALS2-Related Motor Neuron Diseases: From Symptoms to Molecules

*Original*

ALS2-Related Motor Neuron Diseases: From Symptoms to Molecules / Miceli, M., Exertier, C., Cavaglià, M., Gugole, E., Boccardo, M., Rita Casaluci, R., Ceccarelli, N., De Maio, A., Vallone, B., Deriu, M.A.. - In: BIOLOGY. - ISSN 2079-7737. - 11:1(2022), p. 77. [10.3390/biology11010077]

*Availability:*

This version is available at: 11583/2948438 since: 2022-01-07T11:45:10Z

*Publisher:*

MDPI

*Published*

DOI:10.3390/biology11010077

*Terms of use:*

This article is made available under terms and conditions as specified in the corresponding bibliographic description in the repository

*Publisher copyright*

(Article begins on next page)

Received February 7, 2020, accepted February 18, 2020, date of publication February 24, 2020, date of current version March 3, 2020.

Digital Object Identifier 10.1109/ACCESS.2020.2976153

# Generalized Symmetrical 3 dB Power Dividers With Complex Termination Impedances

ANNA PIACIBELLO<sup>1,2</sup>, (Member, IEEE), MARCO PIROLA<sup>2</sup>, (Senior Member, IEEE),  
AND GIOVANNI GHIONE<sup>2</sup>, (Fellow, IEEE)

<sup>1</sup>Department of Electronics, University of Roma Tor Vergata, 00133 Roma, Italy

<sup>2</sup>Department of Electronics and Telecommunications, Politecnico di Torino, 10129 Torino, Italy

Corresponding author: Anna Piacibello (anna.piacibello@polito.it)

**ABSTRACT** The paper introduces a class of two-way, 3 dB narrowband power dividers (combiners), closed on complex termination impedances, that generalizes a number of topologies presented during past years as extensions of the traditional Wilkinson design. Adopting even-odd mode analysis, we demonstrate that, under very broad assumptions, any axially symmetric reactive 3-port can be designed to operate as a 3 dB two-way power divider, by connecting a properly designed isolation impedance across two symmetrically but arbitrarily located additional ports. We show that this isolation element can be evaluated by a single input impedance or admittance CAD simulation or measurement; moreover, an explicit expression is given for the isolation impedance. The theory is shown to lead to the same design as for already presented generalizations of the Wilkinson divider; further validation is provided through both simulated and experimental case studies, and an application of the theory to the design of broadband or multi-band couplers is suggested.

**INDEX TERMS** Power dividers, Wilkinson, hybrid.

## I. INTRODUCTION

Power dividers and combiners are widely adopted in microwave systems, such as power amplifiers. Power dividers provide  $N$ -way splitting of the input signal into output ports that are both matched and isolated with each other, granting at the same time input matching. The same features hold for power combiners, where all ports are matched and the  $N$  input ports are isolated with each other. The two-way, 3 dB Wilkinson power divider [1] is a classical solution to the necessity to have matched and isolated ports while providing a lossless equal power division on a narrow frequency band. Driven by the requirements of various applications, the conventional Wilkinson design has been generalized to provide arbitrary splitting ratio [2]–[4] and phase relation between the output signals [5]–[7]. Additionally, the drive towards system integration has recently made the design of reduced size dividers increasingly popular [8]–[16]. Several techniques have been proposed to this aim, such as the use of defected ground structures [11] and phase shifted transmission lines [14]. Also, the use of transmission lines shorter than the standard quarter-wavelength length is made possible by generalizing the isolation element

with additional lumped or distributed reactive elements [8], [13], [15], by exploiting reactive loading of the transmission lines [10], [12] or by adopting coupled inductors [16]. At the same time, led by increasingly demanding communication standards, research efforts have also addressed the need of broadband [17]–[21], dual-band [22]–[31] and multi-band power dividers [32]–[34]. To enhance the bandwidth, multi-section topologies [17], [19], lumped element implementations [18] and optimized isolation networks [35] have been successfully exploited. In addition, especially for the application to amplifiers, harmonic suppression capabilities have been introduced in the power divider [36]–[38]. We also remark that the design of two-way power dividers is often restricted to real port impedances, although some papers have addressed the case of arbitrary complex impedances [39]–[41]. Finally, a current research driver on the generalization of the Wilkinson topology, related to its miniaturization, is the need of keeping the two output ports physically well separated, while connecting between them a small-size (lumped or distributed) dissipative element requiring, on the contrary, close proximity of the two output divider arms. This problem has been partially overcome by shifting the dissipative element away from the output ports [42] and by introducing short stubs to connect it to the divider arms [43]. While in [42], [43] the

The associate editor coordinating the review of this manuscript and approving it for publication was Wenjie Feng.

overall length of the two arms is still a quarter wavelength, generalizations that allow for shorter arms have also been proposed [8], [9].

The present work generalizes and extends the class of networks that can be adopted as two-way, 3 dB power dividers, matching an arbitrary complex impedance. We demonstrate that, under very broad assumptions (see Section II-C, last paragraph), any lossless 3-port structure with axial symmetry can be exploited to realize a 3 dB narrowband isolating power divider, by connecting a properly designed isolation impedance between two additional ports symmetrically placed in an arbitrary plane orthogonal to the symmetry axis.

We show that the isolation impedance can be directly evaluated, by means of a single simulation or measurement, as the driving point input impedance or admittance between the two aforementioned additional, symmetrically located ports; an explicit expression as a function of the impedance matrix of the resulting 5-port network is also derived.

Concerning input matching, if the structure is chosen arbitrarily, the divider will not be necessarily matched at port 1; however, input matching can be either imposed by design of the 5-port, or obtained by cascading port 1 to a lumped or distributed reactive matching section, without affecting the other properties of the divider, i.e. output matching and isolation.

The proposed theory is a generalization of previous formulations [10]–[16], [18]–[20], [42], [43], whose validity is limited to a specific divider topology, and it enables to exploit arbitrarily complex structures, depending on the targeted application.

The paper is organized as follows. In Section II, the even-odd modal analysis of an axially symmetric structure with an isolation impedance connected between two arbitrarily but symmetrically located ports is exploited to derive the conditions that separately ensure matching and isolation of the divider output ports. It is shown that these conditions can be simultaneously met if the network is reactive and input-matched, and the isolation impedance is the complex conjugate of the driving-point impedance between the two additional ports, measured when the output ports are terminated by their normalization impedances. The analytic expression of the isolation impedance is given. The proposed theory is verified in Section III, where it is applied to the CAD design of an arbitrarily shaped divider structure, and then demonstrated through the design, fabrication and characterization of a more realistic prototype. Its applicability to design broadband or multi-band power dividers is also discussed. Conclusions are finally drawn in Section IV.

## II. ANALYSIS

A reactive, axially symmetric 3-port cannot be simultaneously matched at all ports and have isolated output ports, see [44, Sec. 4.2.1]. In the case of the Wilkinson power divider [1], these conditions can be met by inserting a dissipative element, i.e. a resistor, across the output ports. The traditional  $\lambda/4$  Wilkinson topology can be generalized by

connecting a dissipative element of impedance  $Z_c$  between two extra, symmetrically placed, ports rather than between the output ports [8], [9], [42], [43]. It should be noted that  $Z_c$  is the only dissipative element, while the rest of the structure is lossless, which ensures maximum power transfer between the input and output ports, as required in practical applications.

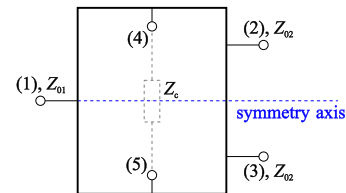


FIGURE 1. Generic axially symmetric 5-port network.

We now demonstrate that any lossless 5-port structure with axial symmetry can be exploited to realize a 3 dB isolating power divider by connecting a dissipative element of impedance  $Z_c$  between two symmetrically placed ports. The 5-port under analysis is depicted in Fig. 1. The input is taken at port 1, while ports 2 and 3 are the outputs, which are symmetrical with respect to the highlighted axis. Ports 4 and 5, between which the complex impedance  $Z_c$  is connected, are also symmetrical with respect to the same axis. The development of the power divider theory for a 5-port rather than a 3-port gives the designer freedom to place the isolation element in the most convenient position, arbitrarily far away from the output ports.  $Z_{o1}$ ,  $Z_{o2}$  indicated in Fig. 1 are the termination impedances of the input port and output ports, respectively, and they can be complex in general. We finally remark that the properties derived in the following have general validity, except for some singular or degenerate 5-ports, which are not practically relevant, as mentioned in II-C.

We perform even and odd mode analysis for a generic axially symmetric reactive 5-port, without reference to any specific topology, adopting a  $Z$  representation. Let us define first the impedances  $Z_{EVEN}$  and  $Z_{ODD}$  seen from either of the output ports under even and odd excitation, respectively, as

$$Z_{EVEN} := \frac{V_2^e}{I_2^e} \tag{1}$$

$$Z_{ODD} := \frac{V_2^o}{I_2^o} \tag{2}$$

see Fig. 2(b)–(c). It should be noted that  $Z_{EVEN}$  does not depend on the isolation element  $Z_c$ , which is not excited, whereas it is affected by the input matching. Conversely,  $Z_{ODD}$  is insensitive to input matching, because port 1 is virtually grounded under odd excitation, but does depend on  $Z_c$ . It follows that the conditions for matching and isolation of the output ports can be derived separately. No other assumption apart from the axial symmetry of the lossless network is made. The circuit to be analyzed is that of Fig. 2(a).

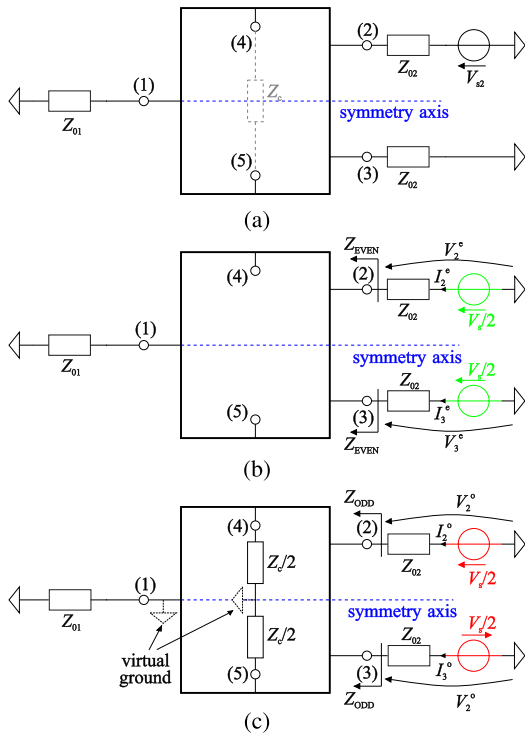


**FIGURE 2.** Generic axially symmetric 5-port excited at port 2 (a) and corresponding even- (b) and odd-mode (c) equivalent circuits.

**A. OUTPUT MATCHING**

Due to symmetry, it is sufficient to impose matching at one of the output ports, e.g. port 2. Connecting a voltage source  $V_{s2}$  to port 2 and decomposing the excitation into even and odd mode excitations at ports 2 and 3, the matching condition at port 2

$$Z_2 = \frac{V_2}{I_2} = Z_{02}^* \tag{3}$$

can be expanded by superposition as

$$Z_2 = \frac{V_2}{I_2} = \frac{V_2^e + V_2^o}{I_2^e + I_2^o} = \frac{V_{s2}}{I_2^e + I_2^o} - Z_{02} = Z_{02}^*. \tag{4}$$

Expressing the even and odd mode impedances defined in (1), (2) in terms of the source voltage

$$Z_{EVEN} = \frac{V_{s2}/2}{I_2^e} - Z_{02} \tag{5}$$

$$Z_{ODD} = \frac{V_{s2}/2}{I_2^o} - Z_{02} \tag{6}$$

and substituting in (4), one obtains:

$$Z_{EVEN}Z_{ODD} + j\Im\{Z_{02}\}(Z_{EVEN} + Z_{ODD}) = |Z_{02}|^2. \tag{7}$$

This output matching condition is here expressed for the first time, as far as our knowledge goes, for a generic 5-port. Equation (7) reduces to  $Z_{EVEN}Z_{ODD} = R_{02}^2$  when  $Z_{02} = R_{02}$  is real.

**B. OUTPUT ISOLATION**

The output ports are isolated if  $V_3 = 0$  when port 2 is excited ( $V_{s2} \neq 0$ ). By superposition of even and odd excitations we obtain

$$V_3 = V_3^e + V_3^o = Z_{EVEN}I_3^e + Z_{ODD}I_3^o = \frac{V_{s2}}{2}Z_{02} \frac{Z_{EVEN} - Z_{ODD}}{(Z_{EVEN} + Z_{02})(Z_{ODD} + Z_{02})}. \tag{8}$$

Since the denominator in (8) is never zero (for passive networks) and the excitation  $V_{s2}$  is non-null, condition

$$Z_{EVEN} = Z_{ODD} \tag{9}$$

must hold to have  $V_3 = 0$ , i.e. the required output ports isolation.

**C. ACHIEVING SIMULTANEOUS OUTPUT MATCHING AND ISOLATION**

Imposing that conditions (7) and (9) be verified simultaneously leads to a second order equation in  $Z_{EVEN}$  (or, equivalently,  $Z_{ODD}$ ) whose solutions are

$$Z_{EVEN1,2} = \begin{cases} Z_{02}^* & (\text{physical, } \Re\{Z_{EVEN1,2}\} > 0) \\ -Z_{02} & (\text{unphysical, } \Re\{Z_{EVEN1,2}\} < 0) \end{cases}. \tag{10}$$

Only

$$Z_{EVEN} = Z_{02}^* \tag{11}$$

is an acceptable solution, since  $\Re\{Z_{02}\} > 0$  by assumption. Taking into account (11) and (9) we finally obtain:

$$Z_{EVEN} = Z_{ODD} = Z_{02}^*. \tag{12}$$

It follows from (12) that output matching and decoupling, together with complete power transfer (through conjugate matching) between the input and output ports can be readily obtained only if the reactive 5-port is input-matched. In fact, let us consider the circuit of Fig. 3, with excitation at port 1, and ports 2 and 3 terminated on  $Z_{02}$ . Since  $Z_c$  it is not excited (and has been therefore replaced by an open) the 3-port connecting port 1 with 2 and 3 is reactive. If port 1 is matched, the power delivered to ports 2 and 3 is, by symmetry, half of the available power at port 1, with no reflections; thus, also port 2 and 3 are matched under even excitation when they are closed on  $Z_{02}$ , leading to (11). The above mentioned conditions are summarized in Table 1.

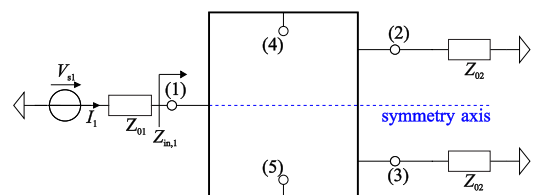


**FIGURE 3.** Generic axially symmetric 5-port network excited at port 1.

Moreover, equation (12) also immediately yields the value of the isolation impedance  $Z_c$ . In fact, assume to apply

TABLE 1. Summary of the design equations.

Equation	Equation No.	Imposed Condition
$Z_{\text{EVEN}}Z_{\text{ODD}} + j \text{Im} \{Z_{02}\} (Z_{\text{EVEN}} + Z_{\text{ODD}}) =  Z_{02} ^2$	(7)	Output matching only
$Z_{\text{EVEN}} = Z_{\text{ODD}}$	(9)	Output isolation only
$Z_{\text{EVEN}} = Z_{\text{ODD}} = Z_{02}^*$	(12)	Conjugate matching at all ports, output isolation

a differential excitation between nodes 4 and 5 when the ports 2 and 3 are closed on their reference impedance  $Z_{02}$ , and take into account that port 1 is connected to a virtual short due to the odd-mode nature of the excitation. Define  $Z_{45}^{o*}$  as the differential impedance seen between ports 4 and 5 under such excitation. Consider the differential (odd-mode) reactive two-port whose input and output ports are between nodes 4-5 and 2-3, respectively. If one assumes that it is output matched, i.e. that  $Z_{\text{ODD}} = Z_{02}^*$  holds when  $Z_c$  is connected across ports 4 and 5, then conjugate matching at the differential port 4-5 must be verified, which implies that the impedance  $Z_c$  to be connected across the differential port 4-5 has value

$$Z_c = Z_{45}^{o*}. \tag{13}$$

To the best of our knowledge, this formalization and generalization of the design principle for 3 dB isolating power dividers had never been derived before.

We finally mention two additional, less practically important, restrictions on the reactive 5-port. Firstly, condition (11) can be realized only if  $Z_{\text{EVEN}}$  has nonzero real part; secondly, condition (13) implies that if  $Z_{45}^{o*}$  has zero real part, also  $Z_c$  is reactive, in contrast with the already mentioned requirement according to which the divider must be dissipative (thanks to the insertion of the isolation impedance) to allow for the isolation of the output ports [44, Sec. 4.2.1]. Thus, both  $Z_{\text{EVEN}}$  and  $Z_{45}^{o*}$  should have nonzero real part. In practice, reactive 5-ports violating either condition are singular (i.e. do not admit a series or parallel representation, or both) or degenerate (e.g. have internally disconnected ports).

**D. EXPRESSING THE ISOLATION ELEMENT**

Representing the 5-port by its Z-matrix, one derives the impedance of the isolation element as

$$Z_c = 2 \left[ Z_{45} - Z_{44} + \frac{(Z_{24} - Z_{25})^2}{Z_{22} - Z_{23} - Z_{02}^*} \right]. \tag{14}$$

The complex impedance can be realized by RC or RL networks, depending on the sign of the reactance, either in series or in parallel. The choice may be driven by bandwidth considerations as well as the feasibility of the component values, depending on the specific case. Assuming an impedance representation with negative reactance, i.e. capacitive reactive elements, the conversion formulas for a series ( $R_{\text{ser}}, C_{\text{ser}}$ ) and a parallel ( $R_{\text{par}}, C_{\text{par}}$ ) network are, respectively,

$$\begin{cases} R_{\text{ser}} = \Re \{Z_c\} \\ C_{\text{ser}} = -1/(\omega_0 \Im \{Z_c\}) \end{cases} \tag{15}$$

$$\begin{cases} R_{\text{par}} = 1/\Re \{1/Z_c\} \\ C_{\text{par}} = \Im \{1/Z_c\}/\omega_0, \end{cases} \tag{16}$$

where  $\omega_0 = 2\pi f_0$ . Similar formulae can be found for  $R$  and  $L$  in case of a positive reactance.

**III. VALIDATION OF THE THEORY**

**A. APPLICATION TO EXISTING DESIGNS**

As a first example, the present theory is applied to some structures taken from the literature, which are all particular cases of the proposed approach. The power dividers proposed in [8], [42], [43] are implemented in a CAD environment, where the impedance  $Z_{45}^o$  defined in Sec. II is computed and  $Z_c = (Z_{45}^o)^*$  is derived hence. In all cases, the method proposed in this paper leads to the same result obtained using the specific formulations from the original works, as summarized in Table 2. Concerning the case in [42], the original paper reports two distinct solutions for the impedance of the isolation element. However, we have shown that the solution should be unique, since it results from imposing a conjugate matching condition. In fact, one of the two solutions in [42] does not allow for exact matching and isolation of the output ports at centerband (see Fig. 3 and 4 in [42]). The solution that we report in Table 2 for comparison is the only one ensuring exact matching and isolation of the output ports.

**B. APPLICATION TO AN ARBITRARILY SHAPED 5-PORT LAYOUT**

As a second, simulated case study, we demonstrate the generality of the present approach by applying the theory to an arbitrarily shaped, axially symmetric structure of size  $(5.5 \times 3) \text{ cm}^2$ , whose layout is shown in Fig. 4(a). Although the selected structure has no equivalent circuit representation, our theory ensures that the problem of finding the isolation impedance has a solution and provides a closed-form expression. The bizarre crocodile-shaped layout has been purposely selected not to target any specific application, but rather to stress the generality of the method. It has been analyzed through electromagnetic simulations adopting ADS Momentum assuming a microstrip FR-4 substrate of 0.8 mm thickness and 4.7 relative dielectric constant; metal and dielectric losses are also considered. The design of the power divider is carried out at the center frequency of 3.5 GHz, assuming a  $50 \Omega$  reference impedance for all ports. The size and shape of the structure are fixed and such that the circuit is not input matched by design; therefore a stub-line input matching network is added at port 1, as shown in Fig. 4(a). The  $Z_c$  impedance value is evaluated from  $Z_{45}^o$  by means of a single

TABLE 2. Application of the proposed method to other works in the literature and comparison of the results.

Reference	Design frequency (GHz)	Configuration	This work			Original work			
			Computed			Computed		Used	
			$Z_c$ ( $\Omega$ )	R ( $\Omega$ )	C (pF)	R ( $\Omega$ )	C (pF)	R ( $\Omega$ )	C (pF)
[43]	1	series	65.99 - j 108.13	65.99	1.47	65.98	1.47	68	1.5
		parallel		243.16	1.07	243.20	1.07	240	1.1
[8]	60	resistor only <sup>a</sup>	50.01 + j 0.01	50.01	-	50	-	50	-
[42]	30	series, $\theta = 65^\circ$	82.14 - j 54.17	82.14	0.098	82.20	0.098	-	-

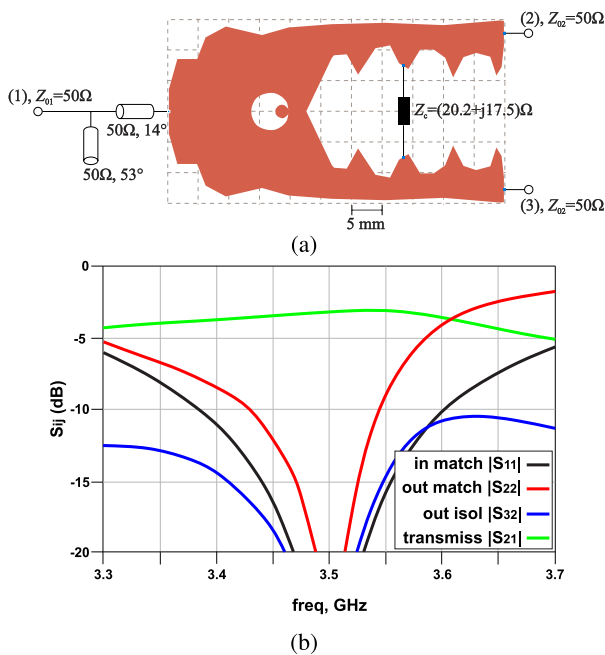


FIGURE 4. Simulation setup for the crocodile-shaped power divider (a). Resulting matching, isolation and transmission (b).

simulation at centerband and results in  $(20.2 + j17.5)\Omega$ . The simulated scattering parameters of the power divider are shown in Fig. 4(b). They demonstrate that an arbitrarily shaped symmetric structure can be used to realize a 3 dB isolated power divider that is simultaneously matched at all ports. Notice the very good matching and isolation at centerband, obtained despite the presence of losses.

C. DESIGN, FABRICATION AND CHARACTERISATION OF A TRANSMISSION-LINE BASED DIVIDER

The proposed approach is now applied to a transmission-line based divider, whose equivalent circuit, layout and photograph are shown in Fig. 5. The topology is inspired by the conventional Wilkinson design, generalized by removing the constraint on the total length of the arms and embedding a bias network into the combiner itself. This is done by adding in the combiner a series dc blocking capacitor  $C_{dec}$ , extra stubs and shunt capacitors  $C_1$ ,  $C_2$  and  $C_3$ . A possible application is in

single-input power amplifiers with two “parallel” branches, such as combined or Doherty amplifiers, which are often based on a Wilkinson configuration; the additional elements are introduced to embed the gate bias networks of the active devices connected at the divider outputs. The divider is designed on  $50\Omega$  at the center frequency of 3.5 GHz and the circuit is fabricated on the same FR-4 substrate considered in Section III-B. The access lines connected to each port have  $Z_{\infty 1} = Z_{\infty 6} = 50\Omega$  and their length is selected to ensure a sufficient distance of the input connector from the circuit ( $\theta_1 = 90^\circ$ ) and required physical separation between the output connectors ( $\theta_6 = 118^\circ$ ). The value of the dc blocking capacitor  $C_{dec} = 47\text{ nF}$  is large enough not to affect the in-band matching, while the shunt capacitors that terminate the stubs are such as to realize a short circuit termination in band ( $C_1 = 15\text{ pF}$ ) and at progressively lower frequencies ( $C_2 = 220\text{ pF}$  and  $C_3 = 1\text{ nF}$ ), thus ensuring for the out-of-band behavior of the bias networks, considering the capacitor parasitics. The parameters related to the divider arms ( $Z_{\infty 2}$ ,  $Z_{\infty 3}$ ,  $\theta_2$ ,  $\theta_3$ ) and stubs ( $Z_{\infty 4}$ ,  $Z_{\infty 5}$ ,  $\theta_4$ ,  $\theta_5$ ) are optimised to ensure input matching ( $S_{11}$  lower than  $-15\text{ dB}$ ) on  $50\Omega$  over a 1 GHz bandwidth around the design frequency. The resulting values are  $Z_{\infty 2} = 66\Omega$ ,  $Z_{\infty 3} = 79\Omega$ ,  $\theta_2 = 48^\circ$ ,  $\theta_3 = 33^\circ$ ,  $Z_{\infty 4} = 90\Omega$ ,  $Z_{\infty 5} = 88\Omega$ ,  $\theta_4 = 82^\circ$ ,  $\theta_5 = 14^\circ$ . The presence of the stubs loading the dividers arms allows to shorten them below  $90^\circ$ . Note that a simpler structure with similar properties (although less flexibility to achieve the desired bandwidth) could have been obtained by imposing  $Z_{\infty 2} = Z_{\infty 3}$  and  $Z_{\infty 4} = Z_{\infty 5}$ . This choice has purposely not been done here because no analytical solution of the equivalent circuit (such as the one performed in [13], [43]) is required, thus allowing to handle a larger number of design parameters with equal ease. Note that, in this initial process, the additional ports 4 and 5 are left open (i.e. not terminated on any impedance). The two additional ports are then considered, and the isolation impedance is evaluated at centerband through simulation. A final optimization is performed to widen the coupler bandwidth, thus obtaining a 10% bandwidth where the port return loss and isolation are better than  $-20\text{ dB}$ . The resulting divider, shown in Fig. 5(c), has size  $4.0 \times 3.0\text{ cm}^2$ .

The design value at centerband of the isolation impedance  $Z_c = (Z_{45}^0)^* = (105.01 - j52.97)\Omega$  is implemented by means of a series RC network, see (15). The ideal values have

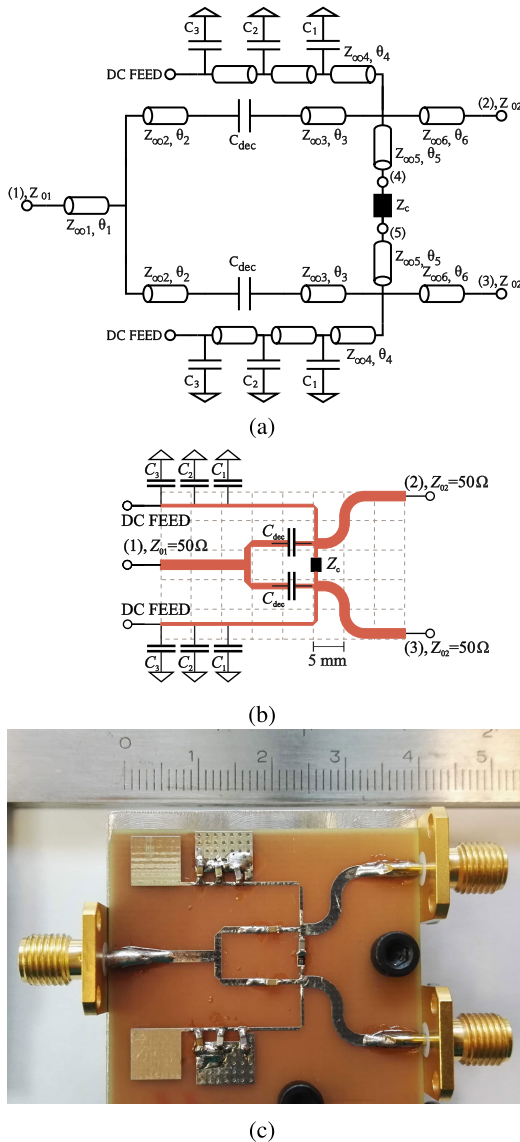


FIGURE 5. Equivalent circuit (a), layout (b) and photograph (c) of the realised demonstrator.

been approximated using SMD components with nominal value  $R_{ser} = 105 \Omega$  and  $C_{ser} = 1.1$  pF.

The experimental characterization is carried out with an Agilent E8361A PNA, calibrated with a 2-port SOLT procedure. The simulated and measured scattering parameters are compared in Fig. 6, before and after the insertion of the isolation impedance. It can be noted that the power divider is input-matched regardless of the presence of  $Z_c$ , as expected. On the contrary, the output ports are neither matched nor decoupled when  $Z_c$  is not present (Fig. 6(a)) and they become so when  $Z_c$  is inserted (Fig. 6(b)). The  $|S_{32}|$  minimum exhibits a slight shift (around 50 MHz) with respect to the design frequency, that is anyway correctly predicted by EM simulations. This shift is probably due to the asymmetry introduced by the physical realization of  $Z_c$ . Realizing the desired  $C_{ser}$  by means of two  $2 C_{ser}$  in series placed on either side of  $R_{ser}$ , may

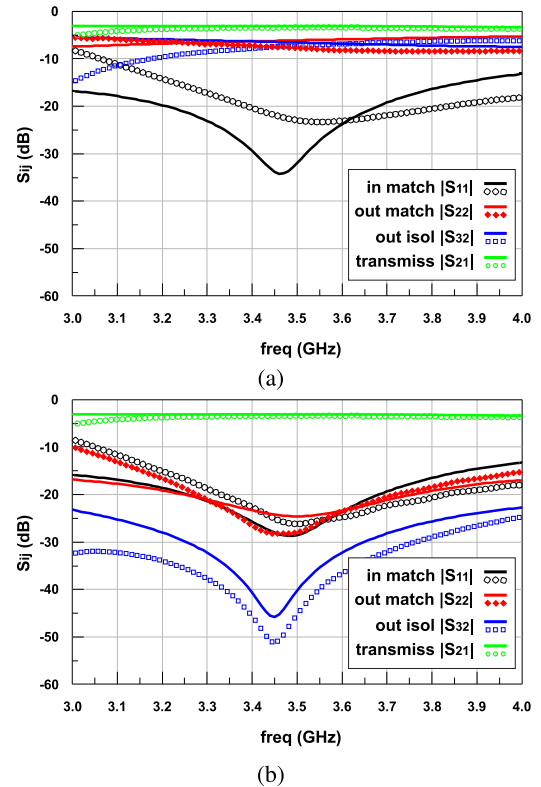


FIGURE 6. Comparison of simulated (solid) and measured (symbols) scattering parameters of the prototype, without (a) and with (b)  $Z_c$ .

improve the layout symmetry, thus minimizing this effect. However, the proposed prototype fully validates the theory and achieves matching and isolation better than  $-20$  dB on a bandwidth in excess of 10% around the design frequency.

#### D. OUTPUT MATCHING TO A COMPLEX IMPEDANCE

As a further demonstration of the validity of the theory, we exploit the prototype design in Section III-C for matching a complex impedance  $Z_{O2} \neq 50 \Omega$  that represents the input impedance of two identical active devices fed by the power divider. Consequently, when referring to the scattering parameters, Kurokawa's definition [45] is assumed. In this case study, we adopt a commercial device, the Cree CGH40006P packaged GaN HEMT. When biased at 28 V drain voltage and 90 mA drain current, and terminated on their power termination, close to  $50 \Omega$ , this devices exhibit an input impedance at 3.5 GHz estimated to be  $Z_G \approx (5 + j12) \Omega$ ; this is the complex value now assigned to  $Z_{O2}$  for the divider design. To design an isolated and matched 3 dB power divider adopting the same 5-port configuration of Section III-C, it is sufficient to estimate the input impedance  $Z_{in,1}$  and the differential impedance  $Z_{45}^0$  across ports 4 and 5. These two operations can be carried out in any order, as one does not affect the other. The simulated values are  $Z_{in,1} = (19.4 - j78.9) \Omega$  and  $Z_{45}^0 = (33.5 - j113.3) \Omega$ . Designing an input matching network to transform the input system impedance ( $50 \Omega$ ) into  $Z_{in,1}^*$  and synthesizing an isolation impedance

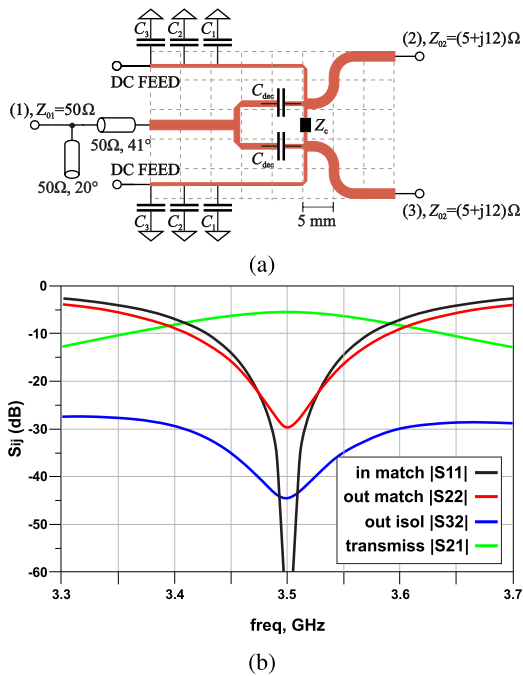


FIGURE 7. Simulation setup for the demonstrator of Section III-C with different port impedance  $Z_{02}$  (a). Resulting simulated matching ( $S_{11}$ ,  $S_{22}$ ), isolation ( $S_{32}$ ) and transmission ( $S_{21}$ ) (b).

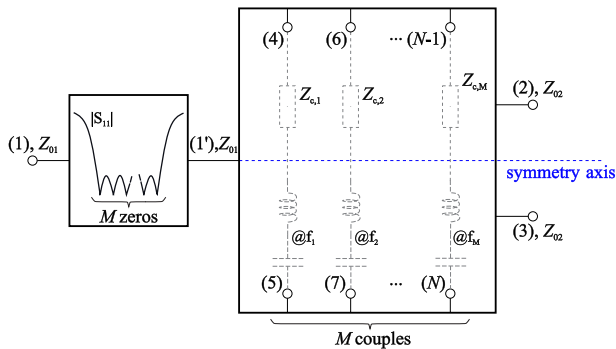


FIGURE 8. Generic axially symmetric  $N$ -port network with  $M$  couples of additional ports and matched at the input port at  $M$  frequencies.

of value  $Z_c = (33.5 + j113.3) \Omega$  to be inserted across ports 4 and 5, automatically ensures that the output ports will be matched and isolated when connected to the input ports of the selected FET. This has been successfully verified in simulation. The resulting circuit is shown in Fig. 7(a) and the corresponding simulated scattering parameters (using as normalization impedances  $Z_{01} = 50 \Omega$  and  $Z_{02} = Z_G$ ) are presented in Fig. 7(b). Notice that the simulated input matching is ideal, due to the external input matching section, while the simulated output matching and isolation, though very good at centerband, are affected by the circuit losses.

### E. EXTENSION TO MULTI-BAND STRUCTURES

Finally, we mention the possibility to extend the proposed theory to the case of multi-band dividers. Referring to Fig. 8, where a generic axially symmetric  $N$ -port is considered, it is

possible to realize a  $M$ -band power divider by considering  $M$  couples of additional ports (4-5, 6-7, ...,  $(N - 1)$ - $N$ ), where  $N = 3 + 2M$ , and connecting across each a distinct isolation element  $Z_{c,m}$  in series to an ideal series resonator at  $f_m$ , which decouples it at all other frequencies, thus making the design of each  $Z_{c,m}$  independent of all others. For the theory to be applicable, input matching must also be ensured at each frequency. This can be done by a matching section (e.g. Chebyshev or Butterworth, not necessarily symmetric) of appropriate order, having  $M$  zeros at the desired frequencies.

### IV. CONCLUSION

We have demonstrated that an arbitrary (non-singular and non-degenerate) axially symmetric reactive structure can be designed to operate as a 3 dB two-way narrowband power divider, thus extending the possible divider topologies beyond the traditional Wilkinson or its generalizations. Matching and isolation of the output ports are achieved by connecting a proper isolation impedance  $Z_c$  between two symmetrically but arbitrarily located additional ports, provided that input matching is also imposed either by design of the reactive structure or by cascading a matching section to its input port. The proposed theory provides a design approach for the isolation impedance with no constraints on the specific topology adopted. A closed-form expression is given for  $Z_c$  in terms of the 5-port parameters; moreover,  $Z_c$  can be also obtained directly by means of a single input impedance simulation or measurement. The theory is validated by applying it to a few case studies, including some of the structures that have been previously presented in the literature, the CAD design through electromagnetic simulation of a divider having arbitrarily shaped symmetric layout, and a more realistic transmission-line divider design on  $50 \Omega$  terminations including the bias networks of the transistors to be connected to the output ports. The divider is realized in hybrid microstrip form; the measured scattering parameters resulting from its characterization confirm the correctness of the approach. As a last example, the same divider was re-designed (with a different isolation impedance and an additional input matching section) on a complex output termination simulating the input impedance of a power transistor; the simulated divider scattering parameters show that the approach is also effective in dealing with complex terminations. Finally, an extension of the theory to the design of broadband or multi-band power dividers is suggested.

### REFERENCES

- [1] E. J. Wilkinson, "An N-Way hybrid power divider," *IEEE Trans. Microw. Theory Techn.*, vol. 8, no. 1, pp. 116–118, Jan. 1960.
- [2] J.-S. Lim, S.-W. Lee, C.-S. Kim, J.-S. Park, D. Ahn, and S. Nam, "A 4.1 unequal wilkinson power divider," *IEEE Microw. Wireless Compon. Lett.*, vol. 11, no. 3, pp. 124–126, Mar. 2001.
- [3] J.-L. Li and B.-Z. Wang, "Novel design of wilkinson power dividers with arbitrary power division ratios," *IEEE Trans. Ind. Electron.*, vol. 58, no. 6, pp. 2541–2546, Jun. 2011.
- [4] R.-F. Tsai, P.-H. Deng, and T.-J. Chang, "A modified unequal wilkinson power divider using T-Shaped transformers," in *Proc. IEEE 20th Electron. Packag. Technol. Conf. (EPTC)*, Dec. 2018, pp. 894–897.

- [5] J.-S. Kim, M.-J. Park, and M.-G. Kim, "Out-of-phase wilkinson power divider," *Electron. Lett.*, vol. 45, no. 1, pp. 59–60, Jan. 2009.
- [6] P.-L. Chi, Y.-W. Chi, and T. Yang, "A reconfigurable in-phase/out-of-phase and power-dividing ratio power divider," in *Proc. IEEE Asia-Pacific Microw. Conf. (APMC)*, Nov. 2017, pp. 287–290.
- [7] H. Zhu, Z. Cheng, and Y. J. Guo, "Design of wideband in-phase and Out-of-Phase power dividers using Microstrip-to-Slotline transitions and slotline resonators," *IEEE Trans. Microw. Theory Techn.*, vol. 67, no. 4, pp. 1412–1424, Apr. 2019.
- [8] S. Horst, R. Bairavasubramanian, M. M. Tentzeris, and J. Papapolymerou, "Modified wilkinson power dividers for millimeter-wave integrated circuits," *IEEE Trans. Microw. Theory Techn.*, vol. 55, no. 11, pp. 2439–2446, Nov. 2007.
- [9] H.-R. Ahn and I. Wolff, "General design equations, small-sized impedance transformers, and their application to small-sized three-port 3-dB power dividers," *IEEE Trans. Microw. Theory Techn.*, vol. 49, no. 7, pp. 1277–1288, Jul. 2001.
- [10] M. C. Scardelletti, G. E. Ponchak, and T. M. Weller, "Miniaturized wilkinson power dividers utilizing capacitive loading," *IEEE Microw. Wireless Compon. Lett.*, vol. 12, no. 1, pp. 6–8, Jan. 2002.
- [11] H. Oraizi and M. S. Esfahlan, "Miniaturization of wilkinson power dividers by using defected ground structures," *Prog. Electromagn. Res. Lett.*, vol. 4, pp. 113–120, 2008.
- [12] C. Miao, J. Yang, G. Tian, X. Zheng, and W. Wu, "Novel sub-miniaturized wilkinson power divider based on small phase delay," *IEEE Microw. Wireless Compon. Lett.*, vol. 24, no. 10, pp. 662–664, Oct. 2014.
- [13] X. Wang, I. Sakagami, A. Mase, and M. Ichimura, "Wilkinson power divider with complex isolation component and its miniaturization," *IEEE Trans. Microw. Theory Techn.*, vol. 62, no. 3, pp. 422–430, Mar. 2014.
- [14] P.-Y. Hsu, K.-H. Lu, C.-H. Lin, A. Liu, and T. Yu, "A 1GHz compact wilkinson power divider based on phase shifted transmission lines," in *Proc. Asia-Pacific Microw. Conf. (APMC)*, Dec. 2016, pp. 1–3.
- [15] T.-J. Chang, T.-J. Huang, and H.-T. Hsu, "Miniaturized wilkinson power divider with complex isolation network for physical isolation," in *Proc. 47th Eur. Microw. Conf. (EuMC)*, Oct. 2017, pp. 396–399.
- [16] C. W. Byeon and C. S. Park, "Low-loss compact millimeter-wave power Divider/Combiner for phased array systems," *IEEE Microw. Wireless Compon. Lett.*, vol. 29, no. 5, pp. 312–314, May 2019.
- [17] S. B. Cohn, "A class of broadband three-port TEM-mode hybrids," *IEEE Trans. Microw. Theory Techn.*, vol. 16, no. 2, pp. 110–116, Feb. 1968.
- [18] Y. Okada, T. Kawai, and A. Enokihara, "Wideband lumped-element wilkinson power dividers using LC-ladder circuits," in *Proc. Eur. Microw. Conf. (EuMC)*, Sep. 2015, pp. 115–118.
- [19] T. Yu, "A broadband wilkinson power divider based on the segmented structure," *IEEE Trans. Microw. Theory Techn.*, vol. 66, no. 4, pp. 1902–1911, Apr. 2018.
- [20] A. Chen, Y. Zhuang, J. Zhou, Y. Huang, and L. Xing, "Design of a broadband wilkinson power divider with wide range tunable bandwidths by adding a pair of capacitors," *IEEE Trans. Circuits Syst. II: Exp. Briefs*, vol. 66, no. 4, pp. 567–571, Apr. 2019.
- [21] H. Oraizi and A.-R. Sharifi, "Design and optimization of broadband asymmetrical multisection wilkinson power divider," *IEEE Trans. Microw. Theory Techn.*, vol. 54, no. 5, pp. 2220–2231, May 2006.
- [22] X. Wang, Z. Ma, and M. Ohira, "Theory and experiment of two-section two-resistor wilkinson power divider with two arbitrary frequency bands," *IEEE Trans. Microw. Theory Techn.*, vol. 66, no. 3, pp. 1291–1300, Mar. 2018.
- [23] M.-J. Park, "Dual-band wilkinson divider with coupled output port extensions," *IEEE Trans. Microw. Theory Techn.*, vol. 57, no. 9, pp. 2232–2237, Sep. 2009.
- [24] Y. Wu, Y. Liu, and Q. Xue, "An analytical approach for a novel coupled-line dual-band wilkinson power divider," *IEEE Trans. Microw. Theory Techn.*, vol. 59, no. 2, pp. 286–294, Feb. 2011.
- [25] I. Sakagami, X. Wang, K. Takahashi, and S. Okamura, "Generalized two-way two-section dual-band wilkinson power divider with two absorption resistors and its miniaturization," *IEEE Trans. Microw. Theory Techn.*, vol. 59, no. 11, pp. 2833–2847, Nov. 2011.
- [26] Y. Wu, Y. Liu, Y. Zhang, J. Gao, and H. Zhou, "A dual band unequal wilkinson power divider without reactive components," *IEEE Trans. Microw. Theory Techn.*, vol. 57, no. 1, pp. 216–222, Jan. 2009.
- [27] N. Gao, G. Wu, and Q. Tang, "Design of a novel compact dual-band wilkinson power divider with wide frequency ratio," *IEEE Microw. Wireless Compon. Lett.*, vol. 24, no. 2, pp. 81–83, Feb. 2014.
- [28] A. Song, X. Wang, Z. Ma, and M. Ohira, "Design theory of dual-band wilkinson power divider with different frequency ratio ranges," in *Proc. Asia-Pacific Microw. Conf. (APMC)*, Nov. 2018, pp. 1489–1491.
- [29] M. H. Maktoomi, D. Banerjee, and M. S. Hashmi, "An enhanced frequency-ratio coupled-line dual-frequency wilkinson power divider," *IEEE Trans. Circuits Syst. II: Exp. Briefs*, vol. 65, no. 7, pp. 888–892, Jul. 2018.
- [30] P. Wen, Z. Ma, H. Liu, S. Zhu, B. Ren, Y. Song, X. Wang, and M. Ohira, "Dual-band filtering power divider using dual-resonance resonators with ultrawide stopband and good isolation," *IEEE Microw. Wireless Compon. Lett.*, vol. 29, no. 2, pp. 101–103, Feb. 2019.
- [31] S.-H. Ahn, J. W. Lee, C. S. Cho, and T. K. Lee, "A dual-band unequal wilkinson power divider with arbitrary frequency ratios," *IEEE Microw. Wireless Compon. Lett.*, vol. 19, no. 12, pp. 783–785, Dec. 2009.
- [32] M. Chongcheawchamnan, S. Patisang, M. Krairiksh, and I. D. Robertson, "Tri-band wilkinson power divider using a three-section transmission-line transformer," *IEEE Microw. Wireless Compon. Lett.*, vol. 16, no. 8, pp. 452–454, Aug. 2006.
- [33] C.-Y. Liou and S.-G. Mao, "Triple-band microstrip wilkinson power dividers with controllable frequency responses," in *IEEE MTT-S Int. Microw. Symp. Dig.*, Jun. 2014, pp. 1–3.
- [34] A. M. Zaidi, M. T. Beg, B. K. Kanaujia, and K. Rambabu, "Hexa-band branch line coupler and wilkinson power divider for LTE 0.7 GHz, LTE 1.7 GHz, LTE 2.6 GHz, 3.9 GHz, public safety band 4.9 GHz, and WLAN 5.8 GHz frequencies," *IEEE Trans. Circuits Syst. II, Exp. Briefs*, vol. 67, no. 2, pp. 275–279, Feb. 2020.
- [35] V. Tas and A. Atalar, "An optimized isolation network for the wilkinson divider," *IEEE Trans. Microw. Theory Techn.*, vol. 62, no. 12, pp. 3393–3402, Dec. 2014.
- [36] K.-H. Yi and B. Kang, "Modified wilkinson power divider for nth harmonic suppression," *IEEE Microw. Wireless Compon. Lett.*, vol. 13, no. 5, pp. 178–180, May 2003.
- [37] D.-J. Woo and T.-K. Lee, "Suppression of harmonics in wilkinson power divider using dual-band rejection by asymmetric DGS," *IEEE Trans. Microw. Theory Techn.*, vol. 53, no. 6, pp. 2139–2144, Jun. 2005.
- [38] R. Mirzavand, M. M. Honari, A. Abdipour, and G. Moradi, "Compact microstrip wilkinson power dividers with harmonic suppression and arbitrary power division ratios," *IEEE Trans. Microw. Theory Techn.*, vol. 61, no. 1, pp. 61–68, Jan. 2013.
- [39] S. Rosloniec, "Three-port hybrid power dividers terminated in complex frequency-dependent impedances," *IEEE Trans. Microw. Theory Techn.*, vol. 44, no. 8, pp. 1490–1493, Aug. 1996.
- [40] H.-R. Ahn and S. Nam, "3-dB power dividers with equal complex termination impedances and design methods for controlling isolation circuits," *IEEE Trans. Microw. Theory Techn.*, vol. 61, no. 11, pp. 3872–3883, Nov. 2013.
- [41] W. Hallberg, M. Ozen, D. Kuylenstierna, K. Buisman, and C. Fager, "A generalized 3-dB wilkinson power Divider/Combiner with complex terminations," *IEEE Trans. Microw. Theory Techn.*, vol. 66, no. 10, pp. 4497–4506, Oct. 2018.
- [42] C. J. Trantanello, "A novel power divider with enhanced physical and electrical port isolation," in *IEEE MTT-S Int. Microw. Symp. Dig.*, May 2010, pp. 129–132.
- [43] X. Wang, M. Ichimura, I. Sakagami, and A. Mase, "Trantanello wilkinson power divider with additional transmission lines for simple layout," *IET Microw. Antennas Propag.*, vol. 8, no. 9, pp. 666–672, Jun. 2014.
- [44] G. Ghione and M. Pirola, *Microwave Electronics* (The Cambridge RF and Microwave Engineering Series). Cambridge, U.K.: Cambridge Univ. Press, 2017.
- [45] K. Kurokawa, "Power waves and the scattering matrix," *IEEE Trans. Microw. Theory Techn.*, vol. MTT-13, no. 2, pp. 194–202, Mar. 1965.



**ANNA PIACIBELLO** (Member, IEEE) was born in Chivasso, Italy, in 1991. She received the bachelor's and master's degrees in electronic engineering and the Ph.D. degree (*cum laude*) in electrical, electronics and communication engineering from the Politecnico di Torino, in 2013, 2015, and 2019, respectively.

In 2017, she was a Visiting Researcher with the Centre for High Frequency Engineering (CHFE), Cardiff University. She is currently a Postdoctoral Research Associate with the Department of Electronics, University of Rome Tor Vergata, Italy. Her current research interests include broadband and highly efficient microwave power amplifiers. Dr. Piacibello was a recipient of the 2018 Young Engineer Prize awarded by the EuMA association.



**MARCO PIROLA** (Senior Member, IEEE) was born in Velezzo Lomellina, Italy, in 1963. He received the Laurea and Ph.D. degrees in electronic engineering from the Politecnico di Torino, Turin, Italy, in 1987 and 1992, respectively.

In 1992 and 1994, he was a Visiting Researcher with the Hewlett Packard Microwave Technology Division, Santa Rosa, CA, USA. Since 1992, he has been with the Department of Electronics and Communications, Politecnico di Torino, Turin, Italy, first as a Researcher and then as an Associate Professor, since 2000. His research interests include the simulation, modeling, design, and characterization of RF and microwave devices and systems.



**GIOVANNI GHIONE** (Fellow, IEEE) was born in Alessandria, Italy, in 1956. He graduated (*cum laude*) in electronic engineering from the Politecnico di Torino, in 1981. Since 1990, he has been a Full Professor in electronics, from 1991 again with the Politecnico di Torino. He has authored or coauthored more than 350 research articles on the above subjects and four books. His research activity has mainly concerned the high-frequency electronics, with particular attention

to the physics-based modeling of compound semiconductor materials and devices and to the design of microwave ICs. He has contributed to the numerical noise modeling and to the thermal modeling of devices and integrated circuits; to the modeling of passive integrated elements, in particular of coplanar components. These activities were later extended to wide-gap semiconductors (SiC, GaN, and related alloys), but also, more recently, to diamond power devices. He is also involved in research on optoelectronic devices, with application to high-speed photodetector and to electro-optic and electro-absorption modulator modeling, more recently within the framework of Si photonics, but also to FIR detectors and to organic and nanodot solar cells. Prof. Ghione was a member of the QPC subcommittee of IEDM, from 1997 to 1998 and from 2006 to 2007, and the Chair, in 2008. He is a reviewer for several international journals and a member of the Editorial Board of the MTT Transactions. He was the EU Arrangement Chair of IEDM, from 2009 to 2010. He also chaired the ED Society Committee on Compound Semiconductor Devices and Circuits, from 2010 to 2015. From 2010 to 2015, he has been an Associate Editor of the IEEE T-ED. He is the T-ED Editor in Chief (2016–2021).

...